Quantification of net vorticity evolution in the left atrium

Prasanta Pal[1], Ziheng Zhang[1], Ben A. Lin[2], Mitchel Stacy[2], Donald Dione[2], Albert J. Sinusas[2], and Smita Sampath[1]

[1]*Diagnostic Radiology, Yale University School of Medicine, New Haven, CT, United States,* [2]*Internal Medicine Cardiology, Yale University School of Medicine, New Haven, Connecticut, United States*

Introduction: Recent studies indicate that up to 25% of patients with heart failure (HF) develop atrial fibrillation (AF). Current imaging markers of LA dilatation and LA fibrosis are detectable only at the late stage of atrial remodeling when irreversible structural changes have occurred. Functional imaging markers of LA remodeling are severely lacking. Differences in LA flow patterns may provide a non-invasive quantitative approach to study LA function and may be detectable early. We have developed a novel
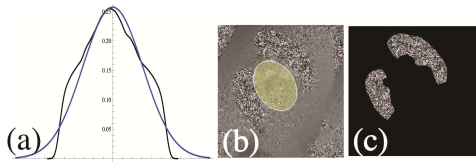

Fig. 1. (a) Noise distribution function (black) of phase contrast velocity data. The blue curve is an overlaid Gaussian distribution function with zero mean and standard deviation 1.55. (b) Phase contrast velocity image. The highlighted region is the approximate region of velocity signal. (c) The masked region is the region where velocity signal amplitude is close to zero.

high temporal resolution magnetic resonance (MR) imaging and image analysis method to quantify vorticity patterns in the left atrium (LA). We hypothesize that alterations in vorticity patterns may provide a quantitative tool to assess early changes in atrial function.

Methods: We have developed an EPI-based high temporal resolution phase contrast MR imaging pulse sequence. This

Fig.2. Vorticity patterns from simulated flow field (V_x= sin(y-1) + 0.5 cos(y), V_y = sin(x-2) + 0.5 sin(y)) in the range $-\pi \leq (x, y) \leq \pi$ depict (a) single large clockwise vortex and four other surrounding small vortices computed with interrogation window N=2, (b) Gaussian noise with standard deviation 0.75 added to both V_x, V_y - Root mean square error (rmse)=0.04, (c) Gaussian filter applied to the noisy data in (b). rmse = 0.0283, (d) Wiener filter applied to (b). rmse=0.025, (e) Total variation filter applied to (b) rmse=0.0296, (f)-(j) similar as in (a)-(e) but the interrogation window N=8. rmse values are (0,0.04,0.0283,0.025,0.0296). In all cases we have chosen appropriate Gaussian, Wiener and Total variation filter parameters. We observe that the vortex looks more spread out and well defined as N gets larger.

sequence was used to acquire LA velocity data in two orthogonal directions on a 4-chamber slice with imaging parameters: imaging matrix: 192×192, resolution: 1.5mm×1.5mm, slice thickness: 8mm, views per cardiac phase: 3, Venc: 120-150 cm/s, temporal resolution: 15ms. The velocity data was filtered using Wiener filters with appropriate averaging radius. The filtered data was used to generate the two-dimensional velocity flow field. Vorticity at every point was calculated from the curl of the velocity field. A finite element
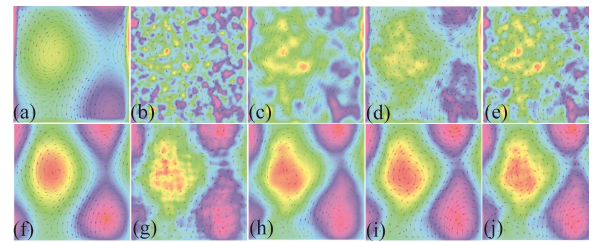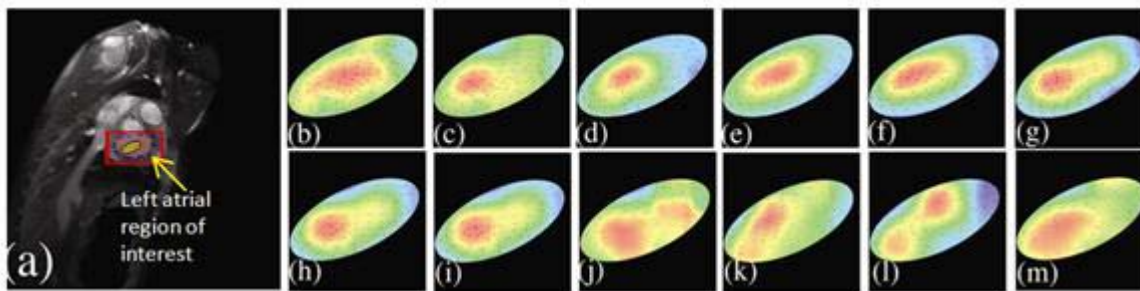

Fig.3. (a) Short axis anatomic view of pig heart. The highlighted region is the left atrium. (b) - (m) Vorticity plot during early systole overlaid with velocity field patterns. Frame (b) is the start of systole and each subsequent frame is separated by 15 ms.

differentiation technique was employed to compute velocity field differentiations using sampled data within a defined interrogation window of optimal size. Positive vorticity values signify counter-clockwise rotation, while negative values signify clockwise rotation. The filter selection and optimal interrogation window size selection was obtained through simulations.

We characterized the noise distribution of the phase velocity data as seen in Fig. 1. By approximating the underlying noise distribution to be Gaussian we have added Gaussian noise to simulated analytical vorticity patterns. To find optimal filter and interrogation window parameters that give the minimal root mean square error (rmse) of the calculated vortex we tested various data filters including Gaussian, Wiener and Total variation and a couple of interrogation window sizes as shown in Fig.2.

Using the optimal filter parameters from the simulation, we computed the vorticity patterns for one normal pig and three pigs at ~8 days post myocardial infarction. To quantify the vortex strength we developed a threshold based vortex segmentation method to segment out the regions having distinct vortices. From the segmented vortices, we calculated the net vorticity over the cardiac cycle.

Results: Simulated velocity fields (streamlines) and their superimposed vorticity color maps obtained using our image analysis methods are shown in Fig (2a)-(2j). Results depict optimal vorticity is obtained using Weiner filter with larger interrogation window. Fig. 3 shows the vorticity patterns for short axis LA view in a normal pig. Atrial vortex is observed during early ventricular systole. The vorticity maps clearly depict the formation and evolution of this atrial vortex. Net vorticity evolution plots are shown in Fig. 4. for one baseline and 3 infarcted pigs. We observe that the vortex strength increases in infarcted pigs. Compared to normal pigs, it also lacks the distinct peaks during early systole and late diastole.

Conclusions: Vortices are formed in the left atrium during early systole and late diastolic periods of the cardiac cycle. These characteristic vortex patterns have been quantified from the 2D flow fields through finite difference curl operator. Through simulations, optimal filter parameters and interrogation window about which vorticity is computed have been determined. The net vorticity plot show visible difference in pattern and magnitude of net vorticity between normal and infarcted pigs.
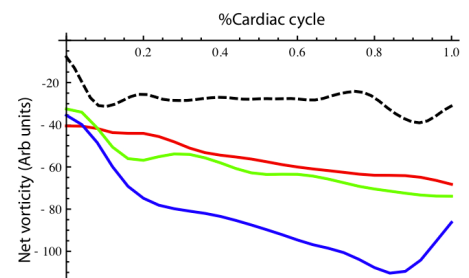

Fig. 4. Net vorticity of the major central clockwise vortex computed from the segmented vortex for normal pig (black dashed line) and ~8 day post infarcted pigs (red, blue, green solid lines).